

A. A. Vovk, I. A. Luchko, G. M. Lyakhov,  
V. A. Plaksii, and N. S. Remez

UDC 532.539+624.131

The aim of many studies in the field of the dynamics of soils, rocks, ice, snow, and other multicomponent porous materials in recent years is construction of models in order to describe wave processes. There appeared to be insufficient foundation for using classical plasticity or linear viscoelastic theory. Experimental study of the propagation and reaction of explosive and weak longitudinal waves, and also deformation of specimens with different loading velocities, shows that the properties of multicomponent porous materials are more varied, and it is necessary to consider them as nonlinear viscoplastic materials with variable viscosity.

On the basis of a model [1] taking account of these properties, a numerical solution is obtained below for the axisymmetric problem of blast-wave propagation in soil. Wave parameters are determined at different distances from the explosion, a dependence is obtained for the intensity of wave extinction on the content of components, and graphs  $p(\epsilon)$  are plotted for volumetric deformation of particles during wave propagation. Results calculated in a computer are compared with test data which confirms the suitability of the model for different soils.

Numerical solution of the problem for spherical blast-wave propagation according to the model in [1] is given in [2], and for deformation of soil with a prescribed variable load it is given in [3]. During numerical solution of the problem use is made of a finite-difference scheme of calculation with artificial viscosity developed for elastoplastic materials [4] and extended to nonlinearly viscoelastic and viscoplastic materials [2].

1. In accordance with the model in [1] soil is considered as a three-component material. The first component is free pore space, filled with air, the second is water, and the third hard mineral particles. We designate with  $\alpha_1$ ,  $\alpha_2$ , and  $\alpha_3$  the initial volume content of the corresponding components,  $\alpha_1 + \alpha_2 + \alpha_3 = 1$ . Compressibility of the first component is determined by the condition for failure and overcompacting of solid and liquid particles under load, and it is considerably less than the compressibility of pore air. Viscous properties and energy dissipation are connected with the instantaneous nature of the overcompacting process and with internal friction. Volumetric strain of the material  $\epsilon$  is determined by volumetric strains for the components  $\epsilon_i$ . We designate  $\rho_0$  as material density and  $\rho_i$  as that of the components:

$$\epsilon = \alpha_1 \epsilon_1 + \alpha_2 \epsilon_2 + \alpha_3 \epsilon_3, \quad \rho_0 = \alpha_1 \rho_1 + \alpha_2 \rho_2 + \alpha_3 \rho_3.$$

Equations for static compression of the components with  $\dot{p} \rightarrow 0$  are approximated by Tate equations:

free pore space

$$p - p_0 = f_S(\epsilon_1) = \frac{\rho_0 C_S^2}{\gamma_S} \left[ (\epsilon_1 + 1)^{-\gamma_S} - 1 \right];$$

rest of the components

$$p - p_0 = \frac{\rho_i C_i^2}{\gamma_i} \left[ (\epsilon_i + 1)^{-\gamma_i} - 1 \right] \quad (i = 2, 3).$$

Here  $p - p_0$  is pressure;  $\rho_i C_i^2$ ,  $\rho_0 C_S^2$  are moduli for volumetric compression of the components. The equation for dynamic compression of the free pore space with  $\dot{p} \rightarrow \infty$  is adopted in the form

$$p - p_0 = f_D(\varepsilon_1) = f_S(\varepsilon_1) + k\varepsilon_1, \quad k < 0.$$

Equations for compressibility of the rest of the components do not depend on loading velocity.

Under these conditions the equation for volumetric compression of the material

$$\dot{\varepsilon} = \frac{\dot{V}}{V_0} = \varphi(p, V) \dot{p} - \frac{\alpha_1 \lambda(p, V)}{\eta} \psi(p, V), \quad (1.1)$$

where

$$\begin{aligned} \varphi(p, V) &= \alpha_1 \left( \frac{df_D}{d\varepsilon_1} \right)^{-1} - \sum_{i=2}^3 \frac{\alpha_i}{\rho_i C_i^2} \left[ \frac{\gamma_i (p - p_0)}{\rho_i C_i^2} + 1 \right]^{-\frac{1+\gamma_i}{\gamma_i}}; \\ \lambda(p, V) &= \frac{df_S}{d\varepsilon_1} \left( \frac{df_D}{d\varepsilon_1} \right)^{-1}, \quad \psi(p, V) = p - p_0 - f_S(\varepsilon_1); \\ \varepsilon &= \frac{V - V_0}{V_0}; \quad V_0 = \frac{1}{\rho_0}; \quad \varepsilon_1 = \frac{1}{\alpha_1} \left\{ \frac{V}{V_0} - \sum_{i=2}^3 \left[ \frac{\gamma_i (p - p_0)}{\rho_i C_i^2} + 1 \right]^{-\frac{1}{\gamma_i}} \right\} - 1; \end{aligned}$$

$\eta$  is volumetric viscosity coefficient.

In the model, consideration is given to different equations for compression and unloading of the free pore space. Equations for compression and unloading of the rest of the components are assumed to be identical. Unloading of the free pore space proceeds according to the relationship

$$\begin{aligned} \varepsilon_1 + 1 &= \left[ \frac{\gamma_R (p - p_0)}{\rho_0 C_R^2} + 1 \right]^{-\frac{1}{\gamma_R}} + \left[ \frac{\gamma_S (p_m - p_0)}{\rho_0 C_S^2} + 1 \right]^{-\frac{1}{\gamma_S}} - \\ &- \left[ \frac{\gamma_R (p_m - p_0)}{\rho_0 C_R^2} + 1 \right]^{-\frac{1}{\gamma_R}}, \quad 1 + \varepsilon_{1m} = \left[ \frac{\gamma_S (p_m - p_0)}{\rho_0 C_S^2} + 1 \right]^{-\frac{1}{\gamma_S}}. \end{aligned} \quad (1.2)$$

Unloading commences when deformation of the free space reaches the maximum value  $\varepsilon_{1m}$ . The equation for volumetric unloading of the material takes the form of (1.1), where

$$\begin{aligned} \varphi(p, V) &= \alpha_1 \left( \frac{df_D}{d\varepsilon_1} - \frac{df_S}{d\varepsilon_1} + \frac{df_R}{d\varepsilon_1} \right)^{-1} - \sum_{i=2}^3 \frac{\alpha_i}{\rho_i C_i^2} \left[ \frac{\gamma_i (p - p_0)}{\rho_i C_i^2} + 1 \right]^{-\frac{1+\gamma_i}{\gamma_i}}; \\ \lambda(p, V) &= \left( \frac{df_D}{d\varepsilon_1} - \frac{df_S}{d\varepsilon_1} \right) \left( \frac{df_D}{d\varepsilon_1} - \frac{df_S}{d\varepsilon_1} + \frac{df_R}{d\varepsilon_1} \right)^{-1}, \quad \psi(p, V) = p - p_0 - f_R(\varepsilon_1); \\ f_R(\varepsilon_1) &= \frac{\rho_0 C_R^2}{\gamma_R} \left[ \left[ \varepsilon_1 + 1 - \left[ \frac{\gamma_S (p_m - p_0)}{\rho_0 C_S^2} + 1 \right]^{-\frac{1}{\gamma_S}} + \right. \right. \\ &\quad \left. \left. + \left[ \frac{\gamma_R (p_m - p_0)}{\rho_0 C_R^2} + 1 \right]^{-\frac{1}{\gamma_R}} \right]^{-\gamma_R} - 1 \right]. \end{aligned}$$

The plasticity condition corresponds to the Mises-Shleicher condition

$$S_r = \frac{k^* (p - p_0)}{1 + \frac{k^* (p - p_0)}{p^* - p_0}}, \quad S_r = \sigma_r + p - p_0, \quad p - p_0 = -\frac{1}{3} (\sigma_r + \sigma_\theta + \sigma_z). \quad (1.3)$$

Values of  $k^*$  and  $p^*$  are determined from experimental values of lateral pressure coefficient  $k_T = \sigma_\theta / \sigma_r$ . It is assumed that radial  $\sigma_r$ , lateral  $\sigma_\theta$ , and axial  $\sigma_z$  stresses are connected by the condition

$$\sigma_z = \frac{1}{2} (\sigma_r + \sigma_\theta). \quad (1.4)$$

Consideration is given below to a Camouflet explosion of a cylindrical charge under conditions that explosive transformations of the explosive and expansion of the detonation products proceeds by a scheme of instantaneous wave detonation. During detonation throughout the whole volume of the charge there is instantaneous establishment of pressure  $p_n$  and detonation product density  $\rho_n$ , equal to the initial explosive density. Subsequently the wave process is considered, including propagation through the soil of the blast wave and rarefaction and compression waves for the detonation products. Expansion of detonation products proceeds by a two-term isentropic equation of state [5-7]

$$p - p_0 = A\rho^n + B\rho^\gamma. \quad (1.5)$$

For trotyl  $\rho_n = 1600 \text{ kg/m}^3$ ,  $Q = 1000 \text{ kcal/kg}$ ,  $n = 3.12$ ,  $\gamma = 1.25$ ,  $A = 0.88 \text{ N/m}^2 (\text{kg/m}^3)^{-n}$ ,  $B = 0.62 \cdot 10^5 \text{ N/m}^2 (\text{kg/m}^3)^{-\gamma}$ .

To describe movement of detonation products use is often made of a single-term isentropic equation of state  $p - p_0 = A\rho^n$ , in which with high explosive product densities  $n = 3$ . However, with considerable expansion the index of the power  $n$  should be reduced by a factor of about two to a value corresponding to rarefied gas. This situation limits use of the latter equation to the high-pressure region. In (1.5) the first term is determining with high pressures, but with low pressures this applies to the second term, which makes it possible to use the equation over the whole process of explosion product expansion.

The main equations of motion for a solid material in Euler variables of  $r$  and  $t$  have the form

$$\begin{aligned} \frac{\partial \rho}{\partial t} + u \frac{\partial \rho}{\partial r} + \rho \frac{\partial u}{\partial r} + \frac{u\rho}{r} &= 0, \\ \rho \left( \frac{\partial u}{\partial t} + u \frac{\partial u}{\partial r} \right) - \frac{\partial \sigma_r}{\partial r} - \frac{\sigma_r - \sigma_\theta}{r} &= 0, \end{aligned} \quad (1.6)$$

where  $u$  is particle velocity.

Relationships (1.1), (1.3), (1.4), (1.6) form a closed set of equations for soil movement. The closed set of equations for detonation product movement includes (1.6) and (1.5).

Initial conditions for the problem are:  $u = 0$ ,  $p = p_n$ ,  $\rho = \rho_n$  for  $0 \leq r \leq r_0$ ;  $u = 0$ ,  $\rho = \rho_0 = 1/V_0$ ,  $p = p$  for  $r_0 < r$ , where  $r_0$  is explosive charge radius. At the boundary of the Camouflet cavity, stress  $\sigma_f$  and velocity  $u$  are constant.

The calculation scheme employed with artificial viscosity using a computer to solve the problem makes it possible to consider relationships at the discontinuity implicitly. The disruption surface is substituted by a transition layer in which values change rapidly but constantly. At the same time, relationships at the shock-wave front remain in force for the transition layer. The stability condition corresponds to the Neuman and Richtmyer modified form of stability [8].

2. Solution is carried out for two soils: sand of average density not impregnated with water and water-impregnated clay. Calculated characteristics for the sandy soil are: density  $\rho_0 = 1660 \text{ kg/m}^3$ , moisture content  $w = 0.12$ ,  $\alpha_1 = 0.3$ ,  $\alpha_2 = 0.18$ ,  $\alpha_3 = 0.52$ ,  $\rho_0 C_S^2 = 9 \cdot 10^6 \text{ N/m}^2$ ,  $k = -4 \cdot 10^7 \text{ N/m}^2$ ,  $\rho_0 C_D^2 = 4.9 \cdot 10^7 \text{ N/m}^2$ ,  $\gamma_S = 10$ ,  $\gamma_R = \gamma_S + 1$ ,  $\eta = 2000 \text{ Nsec/m}^2$ . Clay characteristics are:  $\rho_0 = 2030 \text{ kg/m}^3$ ,  $w = 0.37$ ,  $\alpha_1 = 0.03$ ,  $\alpha_2 = 0.33$ ,  $\alpha_3 = 0.64$ ;  $\rho_0 C_S^2 = 3 \cdot 10^7 \text{ N/m}^2$ ,  $k = -3.7 \cdot 10^9 \text{ N/m}^2$ ,  $\rho_0 C_D^2 = 3.77 \cdot 10^9 \text{ N/m}^2$ ,  $\gamma_S = 4$ ,  $\gamma_R = \gamma_S + 1$ ,  $\eta = 1200 \text{ Nsec/m}^2$ . These values correspond approximately to the parameters of clay in which tests were carried out with cylindrical explosive charges [9].

For both soils it is assumed that  $\rho_2 = 1000 \text{ kg/m}^3$ ,  $C_2 = 1500 \text{ m/sec}$ ,  $\rho_3 = 2650 \text{ kg/m}^3$ ,  $C_3 = 5000 \text{ m/sec}$ ,  $\gamma_2 = 7$ ,  $\gamma_3 = 5$ . Explosive charge radius is 0.1 m.

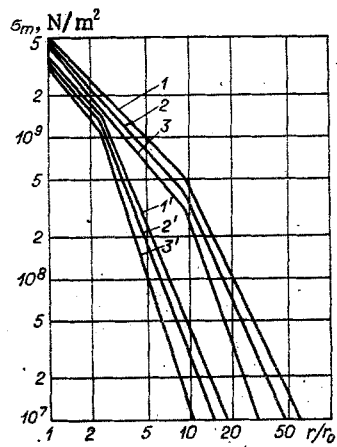


Fig. 1

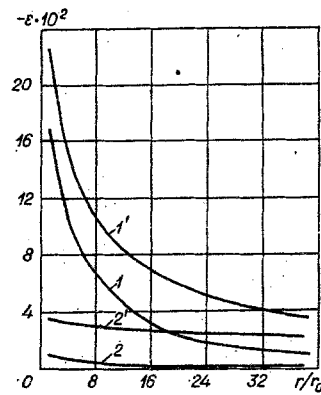


Fig. 2

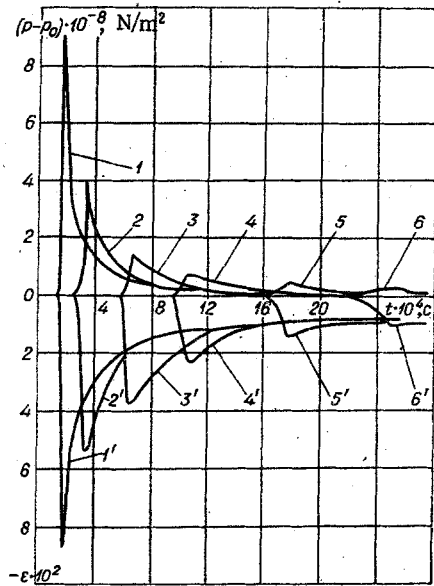


Fig. 3

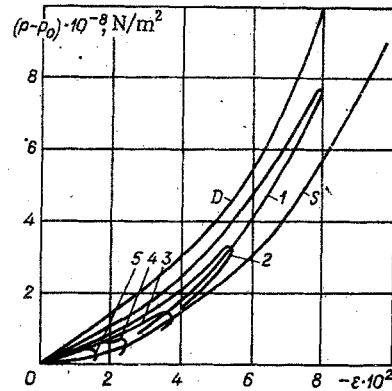


Fig. 4

The coefficient of bulk viscosity is a variable value. Average constant values of it are taken for calculation, selected by analogy with argillaceous and sandy soils [1-6]. Calculations [2] show that a change in  $\eta$  by a factor of 50 changes the main wave parameters with a spherical explosion at distances where maximum stress  $\sigma_r$  is of the order of  $100 \cdot 10^5$  N/m<sup>2</sup> only by a factor of 20-30%.

We now consider the calculated results. Presented in Fig. 1 by lines 1-3 are dependences for maximum values of  $\sigma_r$ ,  $p$ , and  $\sigma_\theta$  on relative distance  $r/r_0$  (here and in Fig. 2 figures without primes correspond to clay, and those with primes correspond to sand). Calculations indicate that wave fading at different distances proceeds with different intensity. The intensity may increase or decrease with distance. In sand not impregnated with water with high  $\alpha_1$  the intensity of fading at all distances is markedly greater than in water-impregnated clay with low  $\alpha_1$ . A similar dependence for wave fading on  $\alpha_1$  corresponds to the tests in [6].

Given in Fig. 2 is the dependence of maximum volumetric strain  $\epsilon_m$  (1 and 1') and residual strain  $\epsilon_R$  (2 and 2') on distance in clay and in sand. In a material with a large volume of free pore space  $\epsilon_m$  and  $\epsilon_R$  are markedly greater at all distances. At short distances in both soils  $\epsilon_m \gg \epsilon_R$ , and at large distances the difference in their values is much less. Close to the gas chamber  $\epsilon_R < \alpha_1$ . With high pressures at the explosive charge boundary after compression there is soil loosening. These results correspond with test data.

Shown in Fig. 3 is the change in pressure and deformation (lines without primes and with primes) with time in particles of argillaceous soil with passage of a wave. Curves 1, 1'-6, 6' relate to  $r/r_0 = 5.47; 9.07; 15.07; 21.07; 30.67$  and  $39$ . Close to the explosive

TABLE 1

$t \cdot 10^{-3}$ , sec	$r_n/r_0$	
	Sand	clay
0,5	2,5	2
1	3,4	2,7
2	4,4	3,4
4	5,4	4,2
6	5,9	4,6
8	6,5	—
10	7	—

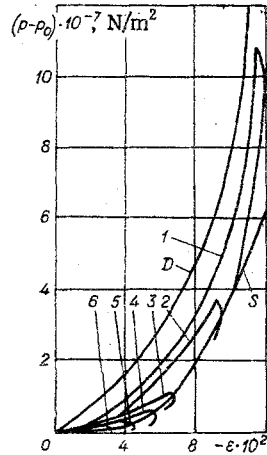


Fig. 5

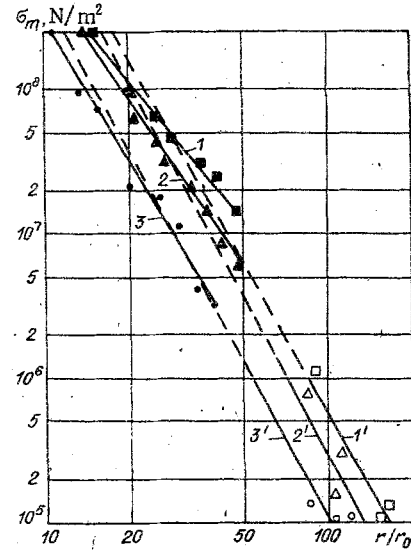


Fig. 6

charge there is an explosive shock wave, and pressure increases by a jump. At a distance from the area of the explosion there is a decrease in pressure, and the time for the increase in pressure to a maximum and its total duration increase. The wave is converted into a continuous compression wave. The decrease in maximum pressure with distance occurs more intensely than for maximum deformation.

In Fig. 4 D and S are limiting dynamic and static curves for volumetric compression of argillaceous soil corresponding to  $p \rightarrow \infty$  and  $p \rightarrow 0$ . Curves 1-5 determine the change in material condition with passage of a wave at the same distances as in Fig. 3. They were plotted from relationships  $p(t)$  and  $\epsilon(t)$  (Fig. 3) with exclusion of time. With increasing distance from the explosion, curves for volumetric compression of particles  $p(\epsilon)$  depart from a dynamic curve and they approach a static curve in conformity with the increase in time for pressure increase.

In Fig. 5 D and S are limiting curves for volumetric compression of sandy soil, and curves 1-5 are for volumetric compression and unloading realized at the same distances as in clay in Fig. 4. Here curves  $p(\epsilon)$  also approach the limiting static curve as distance increases from the point of the explosion. There is a more marked delay in sand than in clay for the development of deformation-related pressure, which is connected with the greater free porosity. Compression curves in clay pass more closely to stress axis than in sand as a result of the lower compressibility of argillaceous soil.

In solving the problem, the change with time of dimensionless gas chamber (cavity)  $r_n/r_0$  was also determined, where  $r_n$  is dimensional radius of the chamber. Calculated results are given in Table 1. The limiting radius in sand and clay is  $\approx 8.5$  and 6.

The volume of the gas chamber depends on soil compressibility; with increasing compressibility it decreases. Limiting values of radius correspond to test data in [6].

Given in Fig. 6 is the dependence of maximum values of principal stresses on distance in argillaceous soil. Curves 1, 1'-3, 3' relate to  $\sigma_r$ ,  $\sigma_z$ , and  $\sigma_\theta$ , and figures without primes correspond to calculations, but those with primes correspond to the experiment [9]. Tests

were carried out in argillaceous soil (Gzhel') with the same constant of components as that assumed in calculations. Experimental points were obtained with  $r/r_0 > 80-90$ , and calculated points with  $r/r_0 < 50$ . For convenience of comparison lines 1'-3' are continued to the calculated points. Comparison points to satisfactory conformity of calculated and experimental results.

The material model [1] reflects the main properties of soils governing their behavior during operation of explosive loads. With its help it is possible to obtain numerical solutions for a number of dynamic problems which are of practical interest. However, for this purpose experimental determination of equations and model constants are necessary for different materials.

The agreement of calculated and test data also indicates that construction of a model for a nonlinear viscoplastic material is possible without introducing functionals governing deformation history. This situation markedly simplifies the solution of dynamic problems.

#### LITERATURE CITED

1. G. M. Lyakhov, Waves in Soils and Porous Multicomponent Materials [in Russian], Nauka, Moscow (1982).
2. A. V. Krymskii and G. M. Lyakhov, "Waves during underground explosions," Prikl. Matem. i Tekh. Fiz., No. 3 (1984).
3. I. A. Luchko, G. M. Lyakhov, V. A. Plaksii, and N. S. Remez, "Modeling in the dynamics of soil not saturated with water by a solid porous multicomponent viscoplastic material," Preprint No. 83.07, Inst. of Strength Problems, Acad. Sci. UkrSSR, Kiev (1983).
4. M. L. Wilkins, "Calculation of elastoplastic flows," in: Computation Methods in Hydrodynamics [in Russian], Mir, Moscow (1967).
5. A. V. Kashirskii, L. P. Orlenko, and V. N. Okhitin, "Effect of the equation of state in the dispersion of detonation products," Prikl. Matem. i Tekh. Fiz., No. 2 (1973).
6. G. M. Lyakhov, Bases of Dynamics for Explosive Waves in Soils and Rocks [in Russian], Nedra, Moscow (1974).
7. F. A. Baum, L. P. Orlenko, K. P. Stanyukovich, et al., Physics of Blasting [in Russian], Nauka, Moscow (1975).
8. R. Richtmayer and K. Morton, Difference Methods for Solving Boundary Problems [in Russian], Mir, Moscow (1972).
9. S. S. Grigoryan, "Study of soil mechanics," Diss. Doc. Phys.-Mat. Sci., MGU, Moscow (1965).